Modeling Methodology for Computing the Radar Cross Section and Doppler Signature of Wind Farms

Laith R. Danoon and Anthony K. Brown, *Member, IEEE*

***Abstract*—Detailed modeling of radar scattering from wind turbines using commercial computational electromagnetic (CEM) tools requires large computing resources and extended run times. This paper will present a dynamic model specifically designed to model the radar cross-section (RCS) of wind turbines and the Doppler signature generated by the rotating blades in a rapid manner. The paper will elaborate on the methodology used for the meshing and the RCS computation of blades, tower and nacelle. Verification of the developed model against measured RCS of canonical shapes is provided. Finally, RCS and Doppler signature results of a generic turbine and a wind farm are presented.**

***Index Terms*—Doppler signature, radar cross-section, wind farm, wind turbine RCS.**

I. Introduction

MANY planning applications for the development of wind farms have been delayed, altered or on some cases rejected based on the concerns of interfering with safety and tracking radars. The complex characteristics of the scattered radar signals from the wind farm may cause degradation of the radar performance near the wind farm area. The large radar returns from wind turbines may reduce the sensitivity over the wind farm area causing small targets to be lost. Furthermore, the movement of the blades generates a Doppler shift that is similar to small aircrafts or commercial airlines on a landing course. This may cause the radar tracker to generate false tracks or alter the track of existing traffic [1]–[3].

The impact of wind farms on radar systems is considered a major concern on a global scale. To develop mitigating solutions, it is necessary to understand the cause of interaction and understand the characteristics of the scattered signal from turbines. This can be achieved through modeling the interaction and identifying the main parameters which cause the radar interference. However, due to the complexity of the problem and its enormous electrical size, modeling the scattering from wind farms has been computationally tedious and requires very large computing resources.

This paper will highlight the main issues concerning the detailed modeling of the RCS of wind turbines using commercial computational electromagnetic (CEM) tools. It will also present a new methodology to model the returns from wind turbines and the Doppler signature generated by the rotating blades in a computationally efficient manner that can be used on standard desktop computers. The verification of the modeled RCS against measured data of canonical shapes and other RCS models are also presented. Finally the paper will demonstrate the models capabilities by modeling the RCS and the Doppler signature of a generic 2 MW wind turbine at selected illumination angles. The presented technique can also be used for large 8 MW turbines with 240 m rotor diameter.

II. Challenges in Detailed Turbine RCS Modeling

Wind turbines are complex in geometry and extend over hundreds or thousands of wavelengths at radar frequencies. Since typical meshing requirements for full-wave electromagnetic solvers to give accurate RCS modeling is 3–8 mesh points per wavelength [4], [5], this makes the computational task of calculating the electromagnetic scattering from wind turbines a challenging one.

Due to the shape and size of wind turbines, the structure must be represented with reasonable geometrical accuracy. Simplifying assumptions regarding the shape and geometry of the turbine components may result in significant RCS variations at radar frequencies. Additionally, the rotation of the blades adds a time dependency that will alter the effective RCS of the turbine for each radar sweep, whereas a longer term variation will occur due to the changes to the wind direction. As a result detailed modeling of the turbine over wide variety of orientations i.e. at different yaw, rotation, blade tilt and blade pitch angles are required in order to obtain representative RCS results.

The modeling work presented in [6] discusses and models the interference caused by wind farms on aviation radars. The study used a commercial CEM tool to calculate the total RCS of the target [7]. Estimated turbine geometry was used, which was based on scaled drawings of a proposed offshore wind turbine and only selected cases of certain rotation and yaw angles were modeled within this work. For the RCS calculation purposes, "the outline was deliberately created in a simple form since generating a detailed model is time consuming, costly... and possibly exceeds the currently available computing power" [6].

The radar studies presented in [8] and [2] included detailed onshore turbine geometry for the RCS modeling. These studies

Manuscript received January 22, 2013; revised April 08, 2013; accepted June 03, 2013. Date of publication August 01, 2013; date of current version October 02, 2013. This work was supported by the EPSRCS's Supergen Wind programme. The Supergen Wind programme is a U.K. wind energy research consortium which was established by the EPSRC on 23 March 2006 and is now in its second phase which started in March 2010.

L. R. Danoon is with the Microwave and Communication Systems (MACS) Research Group, School of Electrical and Electronic Engineering, The University of Manchester, Manchester M13 9PL, U.K. (e-mail: l.rashid@manchester.ac.uk).

A. K. Brown is with the School of Electrical and Electronic Engineering, The University of Manchester, Manchester M13 9PL, U.K. (e-mail: anthony.brown@manchester.ac.uk).

Color versions of one or more of the figures in this paper are available online at http://ieeexplore.ieee.org.

Digital Object Identifier 10.1109/TAP.2013.2272454

used CEM tools [9] and [2], which employ high-frequency RCS approximation methods including, physical optics (PO) integral equations to compute the returns from the surfaces, physical theory of diffraction (PTD) to calculate the contributions from the diffracted fields, and shooting bouncing rays (Ray Tracing) for multiple scattering between components of the turbine. Similarly, [10] used a method-of-moments (MoM) solver and a multilevel fast multipole algorithm (MLFMA) to model the scattering from a detailed turbine geometry and produce an RCS lookup table. In [10] the author states that the model required over 403,600 facets to represent the overall geometry of the wind turbine at the finest grid rendering. Even this number of facets was considered to be not enough to accurately model the scattering from the turbines very large and complex structure. The RCS calculations presented in [2], [8], [10] all required large scale computational resources to run the complete model. In [10], at the lowest frequency, the model took an average of 7 minutes on a supercomputer using 64 or more nodes to complete a single RCS calculation at a given aspect angle [10].

To save time and modeling cost, the results are often given as a table of farfield RCS values at a different of yaw, rotation and pitch angles as given in the previously mentioned studies [2], [6], [8], [10]. The farfield can often be approximated by $2L^2/\lambda$, where L is the dominant dimension length of the object. In the case of the turbine as a whole, farfield distance at 3 GHz corresponds to 362 km (1,210 km at 9 GHz). This is considered to be greater than the maximum operational range of most radars and, therefore, this condition, in practice, is unlikely to be fulfilled. The scattering from a wind turbine may vary significantly with respect to range and the radar antenna pattern at close range [11], [12].

RCS lookup tables often assume a fixed radar height and range, which will give a constant source elevation angle of approximately 0°. This assumption may not be applicable when modeling radars operating near the wind farm or radar systems on moving platforms, such as marine navigational radar or airborne radars. The movement of the radar platform/vessel will cause the source elevation angle to change for each calculation producing different RCS value for each turbine within the wind farm. This adds to the time varying RCS caused by the rotation of the blades. Additionally, when considering airborne radar systems, the scattering contribution due to the ground reflections and the effects of multipath propagation may also significantly alter the scattered field from the turbine. Hence, accounting for the source angle, radar range, the rotation of the blades and the yaw angle will requires impractically large database for general re/use.

When dealing with a large wind farm that comprises of tens or even hundreds of turbines, rather than using the lookup table approach, a fast computational model to predict the RCS of each individual turbine provides a more flexible solution avoiding the limitation associated with lookup tables. Such a solution is presented in this paper in Section III detailing a modeling methodology that allows scenario specific modeling of turbine RCS and Doppler signature. Section IV shows verification of the models against measurements other models. Section V and VI show the modeling results of the static RCS and Doppler signature of an individual turbine and a complete wind farm respectively.

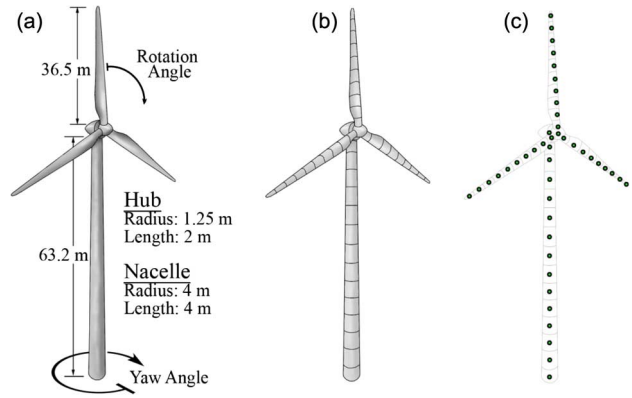

Fig. 1. (a) CAD geometry of a generic 2 MW turbine used in the RCS modeling; (b) segmented turbine for RCS modeling; (c) the RCS point located at center of each segment.

III. RCS Modeling Methodology

When modeling the scattered radar signals from a turbine it is important to address the effect of turbine range, radar antenna pattern, and in some cases the partial shadowing of the turbine due to local terrain [12]. The presented modeling technique requires the turbine to be sectioned into smaller segments such that the radar is in the farfield of each segment but could be in the nearfield of the overall structure. The RCS of each segment is then computed depending on the defined scenario using the methodology given in Section III-A. Fig. 1 shows the modeled 2 MW turbine, the modeling coordinates system and the segmentation.

The blades and the tower of turbine are segmented into multiple small sections along their length. The size and number of segments depends on the application but for a single blade it is typically between 100–200 segments while the tower it is approximately twice the number of segments used in the blade. Once the RCS of each section is computed, the section is then treated as an independent target and its returns to the radar is modeled by accounting for the antenna pattern and other propagation factors. In addition to the static RCS, the segmentation of the turbine enables the modeling of the Doppler signature generated from the rotation of the blades as shown in Section III-B.

A. Segmentation and RCS Modeling

The principle components of a wind turbine (tower, blades and nacelle) are large in wavelength terms and have slow rates of surface curvature. This suggests that meshing the structure into flat facets with sizes greater than 2 wavelengths will approximate the geometry of the structure to reasonable accuracy. Keeping the facet size more than the 2 wavelength enables the use of PO to accurately compute the scattering from each facet using the Stratton-Chu equations for each facet shown in [13]. The use of PO to approximate the RCS of targets has been widely used and well reported in the literature [14], [15]. The presented turbine modeling methodology utilizes this PO approximation in combination with an optimized meshing and segmentation algorithm to model the impact of complete wind farms on a radar system in a dynamic and computationally efficient manner. Reducing the modeling overhead will enable the

study of the wind farm scattering characteristics and assist in the development of mitigation measures.

It is noted that the use of PO to model the RCS will not account for the scattering due to diffraction from sharp edges and wedges. However, since the model was specifically developed to calculate the RCS of predominantly looped curved surfaces on the blades, tower and nacelle; this is not seen to be an area of concern as shown in [21] where the scattering from turbines is dominated by surface scattering.

The meshing of the structure is limited to use quadrilateral facets only. When modeling the blade, for example, quadrilateral meshing can be achieved by aligning the axis of the blade with the Z-axis. The blade length is then sectioned along the Z-axis with a defined section length of no less than 2 wavelengths. Once the sections are digitized, each section is then meshed into small quadrilateral flat facets. A number of these small sections will be grouped together to form a segment, which can then be treated as an independent target as illustrated in Fig. 1(c). The model is referred to as the *Re*ctangular *Me*shing for *R*CS *A*pproximation (ReMeRA) model which is part of the WinR (*Win*d turbine *R*CS) model—a dedicated wind farm impact modeling suit developed at the University of Manchester. Although this paper details the modeling procedure for a generic 36 meter wind turbine blade, the same meshing and RCS modeling procedure is used to compute the scattering from the nacelle or tower by aligning their axis along the Z-axis. Although not explicitly dealt with in this paper this technique can also model the effects on the RCS of blade and tower bending due to wind loading.

The RCS of the segment σ_n, is modeled by computing and adding the scattering from each facet on the segment using the PO formulations in [15]. By default each facet is assumed to be perfect electrical conductor (PEC). If needed, complex composite materials can be approximated by changing the reflection coefficients of the facets.

To obtain the total RCS of the turbine component (blade, tower or nacelle), σ_{TOTAL}, the contributions from all the segments are added coherently. The phase reference point of each segment is assumed to be at the centre of the segment as shown in Fig. 1(c). By defining the location of the radar point and the turbine orientation, the distance to each segment d_n is obtained from the geometry of the scenario. This is then used to compute the phase contribution from each segment. The total RCS of a turbine component, with N segments is obtained using the relative phase method which given by [16]

$$\sigma_{\mathrm{TOTAL}} = \left| \sum_{n=1}^{N} \sqrt{\sigma_n} \exp\left(j \frac{2\pi d_n}{\lambda} \right) \right|^2 \tag{1}$$

For large objects where the RCS is dominated by surface reflection, the relative phase method gives good approximation of the total RCS. However, the relative phase method neglects second order effects such as the mutual coupling between different components of the turbine. Sectioning the turbine into small segments enables the modeling of the turbine's nearfield RCS. This is achieved by coherently adding the farfield RCS from each segment while considering the phase contribution arising from the path length difference from the each segment to the source point. The minimum distance at which the nearfield RCS of the total turbine can be modeled is dictated by the farfield distance of largest turbine segment and the farfield distance of the radar antenna.

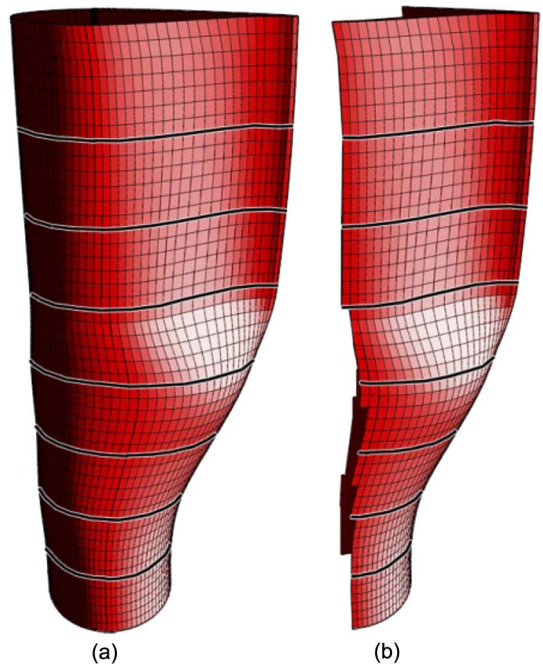

Fig. 2. (a) Segmented blade root with quadrilateral meshing before facet reduction; (b) blade root after meshing and facet reduction due to self-shadowing.

The use of PO approximation in combination with the meshing and segmenting methodology adopted yields to significant reduction in the modeling runtime and computational resources needed. Further improvement to the runtime is achieved through the implementation of simplified shadowing and blade rotation techniques.

Geometrically there are two classes of shadowing. One is where part of the structure is shadowed by different part of the same structure, which in this paper we termed as "self shadowing". This simply means that when incidence angle between the radar source point and the facet normal is more than 90°, the facet is removed from the geometry and no RCS calculations are made for that facet as shown in Fig. 2(b). Although this is a simple approach to the shadowing problem, it significantly reduces the number of facets and hence reduces the run time and the memory usage. For simple shapes the number of facets is usually reduce by a factor of 2.

The second class of shadows is where by a shadow of one component is cast over another component. An example of this is when the blade shadows a portion of the tower or the nacelle. This class of shadowing is termed "component shadowing". This type of shadowing can be included; however, in practice, it is a relatively small and infrequent effect and has a high computational overhead. Therefore, within this paper, only self shadowing is included.

When modeling the rotating blade, a typical calculation may have around 20,000 quadrilateral facets per blade. Rotating the blade geometry, and hence, each point individually using the Euler Rotation Matrix is a significant computational task. Equivalently, it is possible to rotate the source point only to

represent the rotation of the blade. After rotating the source point, the incident angle for each facet is calculated, shadowed facets are removed and the individual RCS of each illuminated facet is computed.

The same fundamental modeling technique can be applied to modeling the tower and nacelle. When modeling the nacelle, component shadowing can only be ignored if the model is limited to computing the RCS of objects with no protruding features that would cast self shadows. This condition is acceptable for most types of nacelles with simple geometries. For nacelle geometries that does not comply with this assumption, simplification of the geometry can be considered as an option since the contribution of the nacelle to the total turbine RCS is small at most incident angles. However, care must be taken when modeling a turbine with a nacelle illuminated from the side (i.e., $\pm 90^\circ$ Yaw). The scattering from the nacelle at such angles may dominate the total RCS of the turbine.

When computing the RCS of each turbine segment, the complex phase and magnitude of the RCS are stored. This then allows the coherent addition of the turbine segments to give the total RCS of the turbine at different rotation and yaw angles.

B. Doppler Signature Modeling

The ReMeRA model can also be used to approximate the Doppler signature generated by the rotating blades. This is achieved by computing the velocity vector and magnitude of each facet on the rotating blade. However, since the ReMeRA model segments the blade into sections along its axis, the facets in each section can normally be assumed to move along the same velocity vector as the blade rotates.

Initially the center point of each blade segment is calculated as the point in the middle of the section as shown in Fig. 3. The centre points are then rotated to the desired orientation by defining the turbines yaw, rotation, tilt and pith angles. To find the direction of movement of each section, the displacement vector, $\boldsymbol{S}$, for each centre is calculated by applying a small rotation increment ΔR (0.5° is a default value) to the defined blade orientation. Then the direction of the section movement, $\hat{s}$, is simply given by normalizing $\boldsymbol{S}$.

Once the movement direction is calculated, the velocity vector of each section $\boldsymbol{V}$, can be calculated using $V = T_s\hat{s}$, Where T_s is the tangential speed of a section L meters away from the blade rotation centre (the hub) as shown in Fig. 3 and given by $T_s = 2\pi L(RPM)/60$, where RPM is the blades rotation rate per minute.

By defining the location of the radar with respect to the turbine, the velocity vector $\boldsymbol{V}$ can be resolved into a scalar value V_r, which is the speed of the section towards or away from the radar point. The Doppler frequency shift f_d, caused by the rotating section can then be calculated using $f_d = 2V_r/\lambda$.

When the Doppler frequency shift is evaluated for each segment, the facets in that segment will be assigned the same value of f_d. The ReMeRA model is then used to calculate the RCS of each segment as described earlier. The output of the model is an array of values for each segment containing its Doppler shift, RCS and phase contribution. In some cases multiple segments may have Doppler shifts that falls within a particular Doppler bin frequency range. The total RCS at that given frequency bin

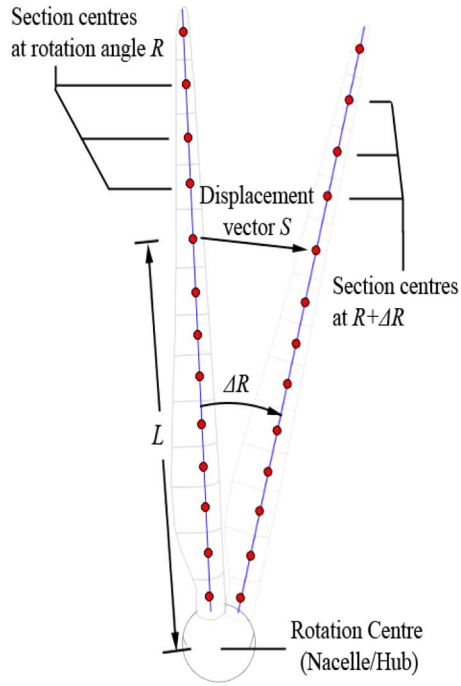

Fig. 3. Displacement vectors of blade section centers for Doppler modeling.

is computed by coherently adding the contribution from each segment as shown previously in (1) while including the change in λ for each segment due to its frequency shift.

The details of the Doppler signature modeling depend on segment length with respect to the blade length and the granularity required for the Doppler calculation. Given a Doppler frequency resolution Δf, the segment length must not exceed ΔL. This is important for side illuminated turbine and for the worst case scenario where V_r is equal to T_s. ΔL can then be derived from the expression relating f_d and T_s as shown above and is given by

$$\Delta f = \left[\frac{2}{\lambda}\right]\left[\frac{2\pi\Delta L(RPM)}{60}\right] \tag{2}$$

$$\Delta L = \frac{15\Delta f\lambda}{(RPM)\pi} \tag{3}$$

IV. RCS Verification

The geometry of the principal turbine components primarily consists of large flat areas and slow curving surfaces. Therefore, it is important be able to accurately and efficiently model the reflected signal of such large surfaces. The ReMeRA model was extensively tested against measured RCS data of canonical shapes with flat and curved surfaces. To further test the ReMeRA model ability to model turbine components, it was compared against FEKO [17].

It is worth noting that RCS measurements may be conducted in an anechoic chamber and the nearfield data is extrapolated to farfield RCS. The accuracy of the RCS measurement is dictated by the size of the tested target in comparison to the size of the test chamber. The RCS of larger targets cannot be measured in small chambers as these nearfield to farfield approximations would fail. Although testing the ReMeRA model against measured data for large objects is more appropriate, no available

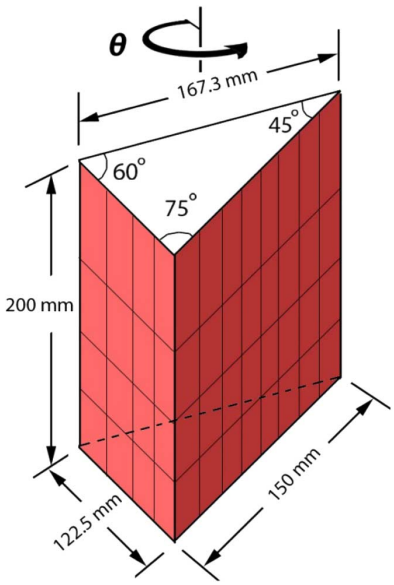

Fig. 4. Geometry of the prism used in the validation of the ReMeRA model.

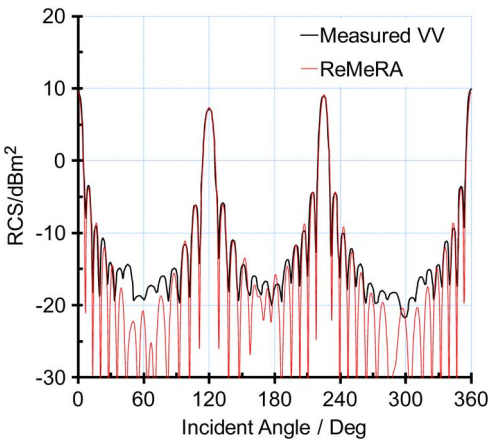

Fig. 5. ReMeRA model versus measured RCS pattern of the prism measured at 8 GHz with vertical polarization [18].

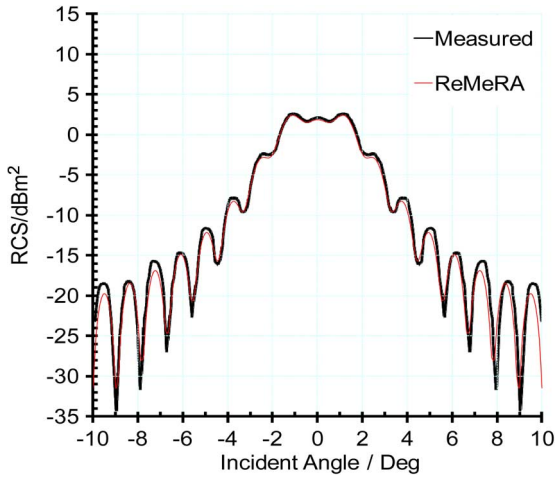

Fig. 6. ReMeRA model versus measured nearfield RCS pattern of the cylinder measured at 12 GHz [19].

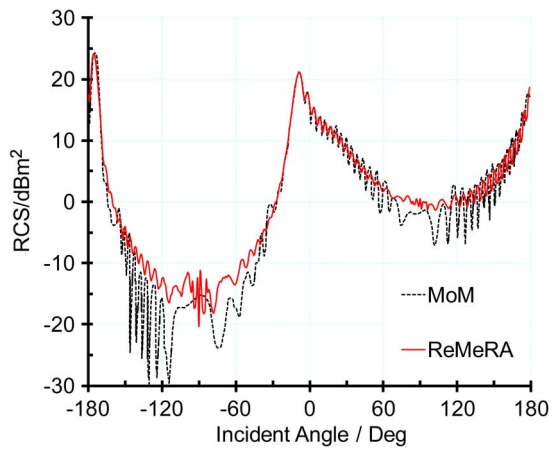

Fig. 7. Modeling data comparing results from RECOTA [15], Method of Moments and ReMeRA at 16 GHz for a NACA-3317 profile.

data was found at the due to the difficulty and the lack of facilities to measuring the RCS of large structures.

A. Verification Against Measurements

The model was verified against measured farfield RCS data of a prism [18] shown in Fig. 4 and nearfield RCS of a upright cylinder with 127 mm diameter and 631.8 mm length as given in [19]. The prism and the cylinder were modeled at 8 GHz and 12 GHz respectively. Both shapes were segmented along its axis and applied the faceting approach detailed in Section III. The modeled farfield RCS of the prism is shown in Fig. 5 while the nearfield RCS of the cylinder is shown Fig. 6.

The ReMeRA model shows an excellent correlation around the specular region in both cases. The model accurately predicts angles and the levels of the specular reflections. The levels of the peak values are within 0.1 dB of the measured data. As the incidence angle moves away from the specular angle the correlation remains good although loses some accuracy when the scattering through diffracted waves from the edges becomes more apparent on the total RCS as noted in Fig. 5. The ReMeRA model is based purely on PO approximation and does not account for the diffracted fields; therefore, at incident angles illuminating the edges of the prism the RCS predictions are lower than the measurements. As the total RCS of the turbine is dominated by surface scattering such differences are deemed to be acceptable for the purpose of this model [21].

B. Verification Against Models

Since the wind turbine blades are made of different airfoil profiles along its length, the RCS of airfoils is of particular interest. Although no measured data was available for the verification process at the time, the modeling work presented in [15] was used to cross examine the ReMeRA model's ability against modeling using the Method of Moments (MoM). A four digit NACA 3370 airfoil profile with a chord length of 150 mm and a section length was 760 mm was modeled at 16 GHz. The results are shown in Fig. 7.

The ReMeRA does not account for the diffraction from the trailing edge or the impact of second-order scattering terms, such as, creeping waves around the leading edge, travelling waves from the trailing edge, or tip-to-tip interactions on the overall RCS predictions. Given this the developed model

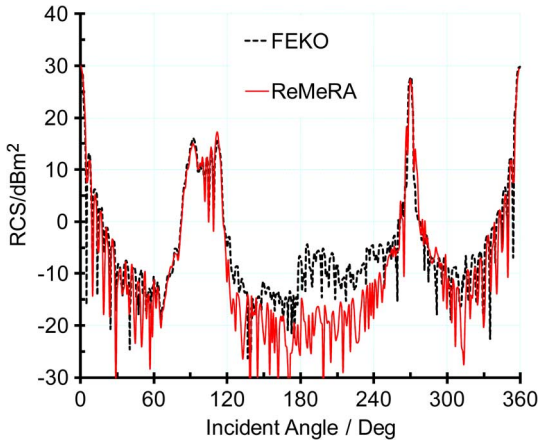

Fig. 8. ReMeRA versus FEKO RCS results at 1 GHz.

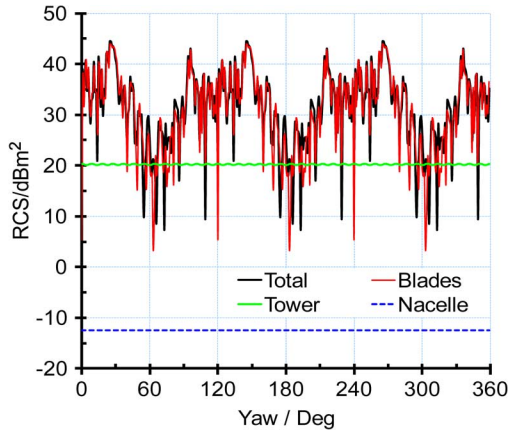

Fig. 9. Turbine RCS over a complete rotation at yaw $= 0°$.

showed excellent correlation with the Method of Moments for this size of object.

The ReMeRA was also compared against the RCS modeling results obtained from FEKO for a full wind turbine blade. FEKO uses a combination of techniques to calculate the electromagnetic scattering of large target [17]. In the case of modeling the scattering from this wind turbine blade, hybridized PO/MoM and UTD/MoM techniques were used to model the total RCS.

Although the blade is usually modeled as a hallow PEC shell, for the purpose of this verification, the blade root was closed by attaching a circular disk at the point of attachment with the hub. This will give a closed blade geometry which will speed the modeling runtime within FEKO. The RCS was modeled at 1 GHz. A vertical cut was taken around the blade starting by illuminating the blade root-cap, then varying the incident angle to illuminate the trailing-edge, blade-tip, leading-edge and then back to the root-cap. The results are shown in Fig. 8.

The results are in very good agreement with both the levels and positions of the RCS peaks. The difference between the two models noted at 180° is when the tip of the blade is illuminated. This is due to the contribution of the diffracted waves to the RCS of the total blade. It is worth noting that for the RCS of a complete wind turbine, this will not be a concern as the RCS will be dominated by other parts of the structure such as the reflections from the other blades, the tower or the nacelle.

The good agreement with the measurements and results from other models gives confidence that the ReMeRA model can predict the RCS of turbine components to a good level of accuracy.

V. Turbine RCS Results

The developed model was used to model the total RCS of a generic wind turbine generated within the Supergen Wind research programme [20]. The general turbine geometry and modeling orientation is shown in Fig. 1. A tilt angle of 5° is applied to the blades to provide sufficient clearance distance between the rotating blades and the tower. For the purpose of this paper, the radar is placed within the farfield of the turbine and the turbine is assumed to be rotating at 15 RPM. Furthermore, the turbine structure is assumed to be a PEC shell and the RCS results were modeled at 3 GHz.

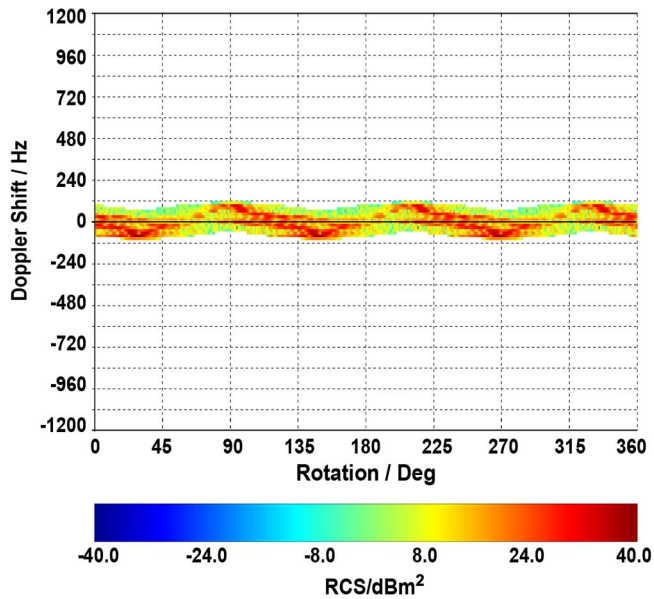

Fig. 10. Doppler signature of the turbine blades at 0° yaw.

The highest RCS profile is expected to occur when the turbine is facing the radar. This is due to the illumination of the large and relatively flat pressure-sides of the blades. Fig. 9 shows the total turbine RCS generated over one full rotation. Fig. 9 also shows the RCS of each component individually. The runtime required to generate 360 calculations to represent a full rotation was approximately 2 minutes on a standard desktop machine.[1]

The results show that for this particular turbine geometry, the contribution from the cylindrically tapered tower is 20 dBm^2, which will be constant at all yaw angles. The blades are the dominant contributor to the total RCS at this illumination angle reaching peak values of 44 dBm^2. At this yaw angle, the Doppler is low as the blades are not moving significantly in the direction of the radar. Fig. 10 shows the Doppler signature generated by the blades at 0° yaw. Only the contribution from the blades are modeled as the tower and the nacelle are assumed to be static and are not moving or vibrating as the blades rotate.

Although the RCS levels are high reaching up 40 dBm^2, the Doppler shift is relatively low and is confined between

[1]Desktop PC with AMD Phenom ii $\times 6$ 3.2 GHz processor and 4 GB of RAM

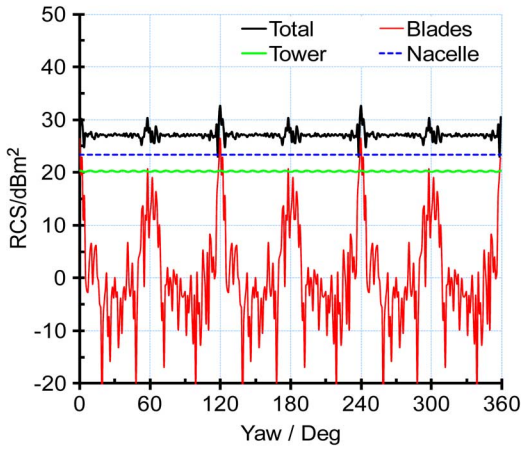

Fig. 11. Turbine RCS over a complete rotation at yaw $\pm 90°$.

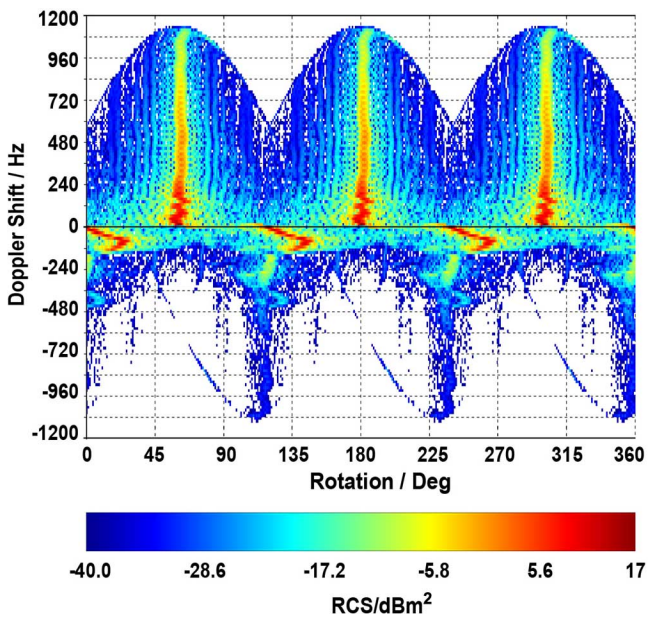

Fig. 12. Doppler signature of the turbine blades at $\pm 90°$ yaw.

± 120 Hz. This is caused by the tilt applied to the blades to avoid collision with the tower, which generates a slight movement towards/away from the radar as the blades rotate. The runtime required to generate the Doppler signature for the three blades across the full rotation (360 points) was approximately 2.6 minutes.

The illumination of the side of the turbine is considered to be the worst case scenario for Doppler based radar systems. Therefore, the ReMeRA model was used to predict the RCS of the turbine at 90° yaw. The results of the static RCS profile are shown in Fig. 11 while the Doppler signature from the blade is shown in Fig. 12.

The static RCS of the turbine is dominated by returns from the nacelle at most rotation angles. The tower is also contributing significantly to the total RCS while the blades are only flashing when the leading-edge of a blade is illuminated. The Doppler plot shows that maximum Doppler shift caused is ± 1100 Hz. The illumination of the leading-edge generates high return with a high Doppler shift. When the trailing edge is illuminated, the high returns are generated by the cylindrical root section of the blade which does not contribute to the high Doppler returns. This compares well with Doppler signature measurements as shown in [2].

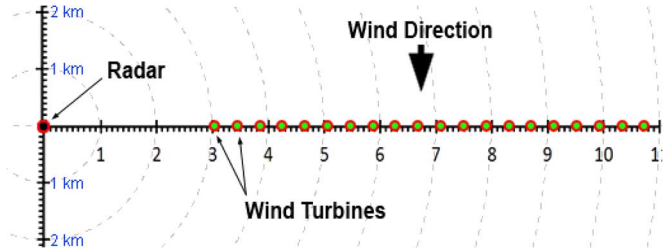

Fig. 13. Modeled wind farm layout and wind direction with respect to radar.

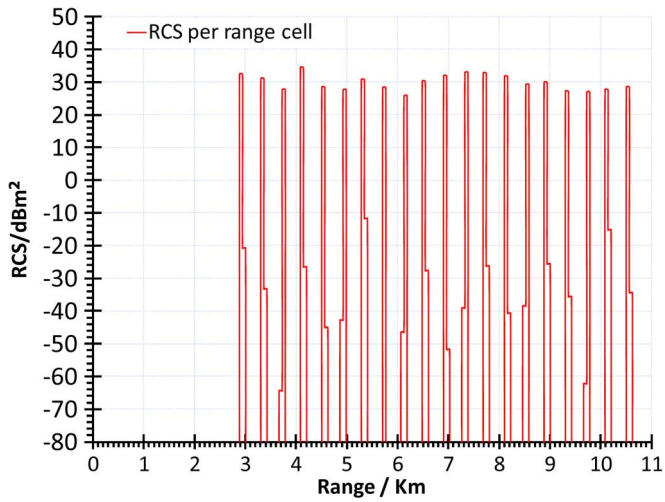

Fig. 14. Modeled wind farm's effective static RCS in each range-cell.

VI. RCS of Wind Farm

This modeling methodology was developed to enable the rapid assessment of the impact of a complete wind farms on radar using a standard desktop computer. To demonstrate this, the RCS of a wind farm with 20 turbines placed on a straight line was modeled. All the turbines in the wind farm were assumed to have the same generic geometry as Fig. 1. The modeling layout of the wind farm with respect to the radar is shown in the PPI illustrated in Fig. 13.

The wind direction was chosen to produce a 90° yaw angle with respect to the radar. Additionally, to account for the variation in each of the turbines Doppler returns the rotation of each turbine was chosen at random between 0°–120°. The RCS of the wind farm was modeled assuming a radar operating at 3 GHz and an effective range-cell length of 60 m. For the purpose of this paper the RCS was modeled including the effect of the radar antenna pattern and the effect of propagation over the sea surface but excluding inter-turbine shadowing. The modeled results show the effective RCS at each radar range cell obtained by coherently summing the contributions from each turbine segment in that range-cell. The modeling results of the static RCS are shown in Fig. 14 while the RCS with the Doppler shift is shown in Fig. 15.

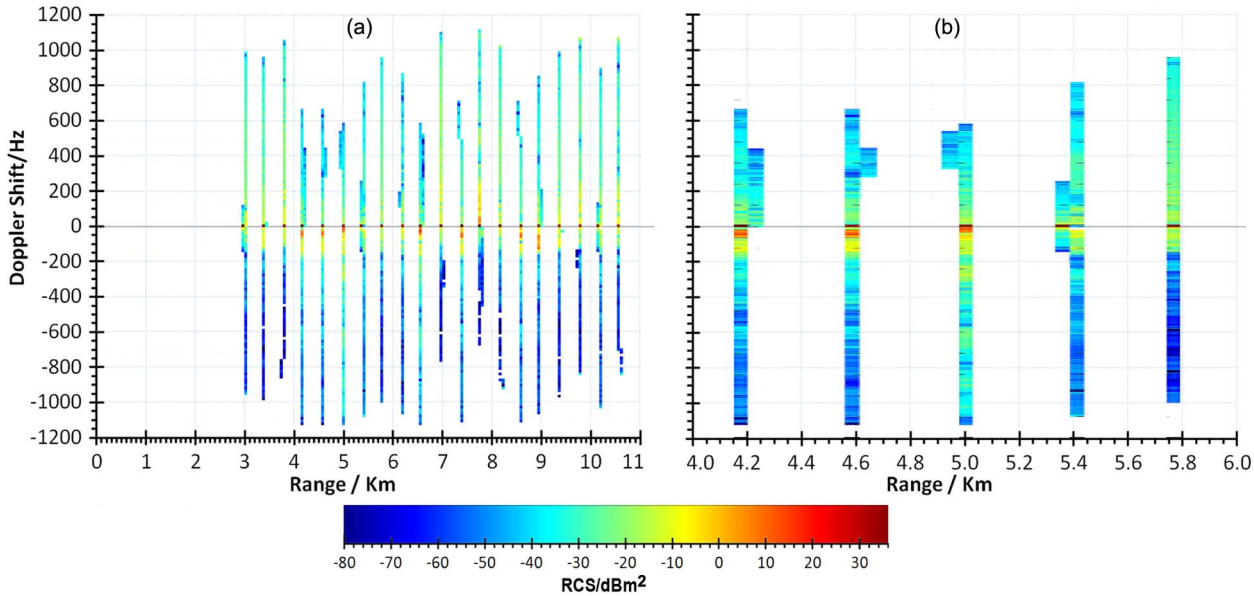

Fig. 15. RCS and Doppler shift of (a) the modeled wind farm (b) the turbines between the ranges of 4 to 6 km.

The rotor diameter of the modeled turbines is 78 m while the radar range-cell length, which is dependent on the pulse width, was assumed to be 60 m. As the rotor diameter is larger than the range-cell length the turbine structure will fall within multiple range-cells simultaneously. This can be noted in Fig. 14 which shows that the RCS profile for each turbine occupies two adjacent range-cells. The peak RCS for each turbine is within the range-cell where the tower and nacelle are located as the returns from the tower and nacelle dominate the turbine RCS at this yaw angle as shown in the previous section.

Fig. 15 shows that the RCS levels and the Doppler signature vary for each modeled turbine due to the randomized blade rotations of the turbines. The results also show that strong RCS component is at 0 Hz Doppler generated from the tower and nacelle (illustrated in Fig. 15 by the dark red point in each range-cell). The blade contributes significantly when the leading-edge is illuminated producing a high positive Doppler shift. Additionally, the Doppler signature generated from each turbine extends over two range-cells as shown in the static RCS profile. It is noted that the returns from the adjacent cell is low (approximately -15 to -70 dBm^2) for this particular turbine geometry. This is the result of only a small portion of the blade near the tip appearing the adjacent range-cell.

However, for turbines with rotor diameters that are considerably larger than the cell length returns from adjacent cells will be higher (as high RCS sections of the blade will be in that cell) and may then impact on the radar tracking performance.

Using the ReMeRA modeling methodology presented in this paper, the modeling time taken to complete the static RCS and Doppler signature for this specific scenario was 11.7 seconds while the modeling runtime for a larger wind farm with 80 turbines was 42.9 seconds. This rapid modeling runtime gives flexibility and enables the study of the impact of wind farms on different radar systems under various scenarios without the need for supercomputing environments.

VII. Conclusion

The interaction between wind farms and radar systems is complex in nature due to the various parameters affecting the scattering behavior of turbines. Modeling the RCS of wind turbines and is often considered a computationally challenging task due to the electrical size of the turbines in comparison to the radar wavelength. Although it is possible to compute the RCS of wind turbine using standard CEM tools, the computational requirements may include supercomputing environment and extended runtimes. To efficiently use the computing resources, it might be possible some cases to run the models and compile a large lookup table with farfield RCS values of the turbine at different orientations and rotation angles. But in the cases where the radar is operating near the wind farm farfield RCS will not give accurate representation of the turbine scattering. Hence, accounting for the source angle, radar range, the rotation of the blades and the yaw angle will requires impractically large lookup tables.

The developed turbine modeling methodology uses a simplified meshing and segmentation to enable the computation of the turbine RCS at different ranges and orientations. The use of PO formulations combined with the meshing, shadowing and rotation of turbine components gave results of good accuracy compared to other models and measured data. The RCS levels were in excellent agreement over the peak values and the regions where the RCS is dominated by surface reflections. Given the large size and the slow rates of curvature of wind turbine components this is valid for large range of practical cases. The runtime was typically few seconds per turbine orientation on a standard desktop environment.

The model was extended to compute the RCS and Doppler signature of complete wind farms. In this paper we consider a 20 and 80 turbine wind farms. Both RCS and Doppler signature were computed within tens of seconds of runtime.

ACKNOWLEDGMENT

The authors would like to thank the members of the former DTI's Stealth Technology for Wind Turbines consortium.

REFERENCES

[1] N. T. Jago, Wind Turbines and Aviation Interests—European Experience and Practice, ETSU W/14/00624/REP, DTI PUB URN No. 03/515, 2002.

[2] G. J. Poupart, Wind Farms Impact on Radar Aviation Interests DTI report number W/14/00614/00/REP, Sep. 2003, BWEA Radar Aviation Interests Rep..

[3] Wind Energy, Defence & Civil Aviation Interests Working Group, Wind Energy and Aviation Interests—Interim Guidelines, ETSU W/14/00626/REP, Oct. 2002.

[4] F. Costen, J. P. Brenger, and A. K. Brown, "Comparison of FDTD hard source with FDTD soft source and accuracy assessment in Debye media," *IEEE Trans. Antennas Propag.*, vol. 57, no. 7, pp. 2014–2022, Jul. 2009.

[5] D. B. Davidson, *Computational Electromagnetics for RF and Microwave Engineering*. Cambridge, U.K.: Cambridge Univ. Press, 2005.

[6] M. M. Butler and D. A. Johnson, Feasibility of Mitigating the Effects of Wind Farms on Primary Radar Alenia Marconi Systems Ltd., 2003.

[7] S. H. W. Simpson, P. Galloway, and M. Harman, "Applications of epsilon a radar signature prediction and analysis tool," presented at the Int. Radar Symp., Munich, Germany, 1998.

[8] M. Bryanton *et al.*, Stealth Technologies for Wind Turbines Final Report, BAE, Rep. No: TES101865, Dec. 2007.

[9] D. P. Allen *et al.*, MITRE RCS Calculation Capability, 1994, MITRE Corp..

[10] B. M. Kent *et al.*, "Dynamic radar cross section and radar Doppler measurements of commercial general electric windmill power turbines part 1: Predicted and measured radar signatures," *IEEE Antennas Propag. Mag.*, vol. 50, no. 2, pp. 211–219, Feb. 2008.

[11] A. C. K. Thomsen *et al.*, "Air traffic control at wind farms with TERMA SCANTER 4000/5000," in *Proc. IEEE Radar Conf.*, Aug. 2011, pp. 247–255.

[12] G. Greving, W. D. Biermann, and R. Mundt, "On the relevance of the measured or calculated RCS for objects on the ground-case wind turbines," presented at the 3rd Eur. Conf. Antennas and Propagation, 2009.

[13] E. F. A. S. Knott and J. F. M. T. Tuley, *Radar Cross Section*, 2nd ed. Boston, MA: Artech House, 1993.

[14] D. C. Jenn and M. F. Chatzigeorgiadis, "A MATLAB physical-optics RCS prediction code," *IEEE Antennas Propag. Mag.*, vol. 46, no. 4, pp. 137–139, Aug. 2004.

[15] N. N. Youssef, "Radar cross section of complex targets," *Proc. IEEE*, vol. 77, no. 5, pp. 722–734, May 1989.

[16] J. W. Crispin,, Jr. and A. L. Maffett, "Radar cross-section estimation for complex shapes," *Proc. IEEE*, vol. 53, no. 8, pp. 972–982, Aug. 1965.

[17] D. B. Davidson *et al.*, "Recent progress on the antenna simulation program FEKO," presented at the South African Symp. Communications and Signal Processing, 1998.

[18] D. Escot-Bocanegra *et al.*, New Benchmark Radar Targets for Scattering Analysis and Electromagnetic Software Validation, 2008, Instituto Nacional de Técnica Aeroespacial. Madrid, Spain, pp. 40–51.

[19] D. G. Falconer, "Extrapolation of near-field RCS measurements to the far zone," *IEEE Trans. Antennas Propag.*, vol. 36, no. 6, pp. 822–829, Jun. 1988.

[20] Supergen, Supergen Wind Energy Technologies Consortium (Supergen Wind), Jul. 2009, cited [December] [Online]. Available: http://www.supergen-wind.org.uk

[21] J. Pinto, J. C. Matthews, and C. Sarno, "Radar signature reduction of wind turbines through the application of stealth technology," in *Proc. Antennas and Propagation Conf.*, Mar. 2009, pp. 3886–3890.

Laith R. Danoon, photograph and biography not available at the time of publication.

Anthony K. Brown, photograph and biography not available at the time of publication.